Ind. J. Pharm. Edu. Res., 2026; 60(3):1199-1205.
https://www.ijper.org

Original Article

Investigation of Potential of *Oxalis corniculata* through Inhibition of Matrix Metalloproteinases for the Treatment of Skin Photoageing: An *in silico* Approach

Madhuri Baghel[1,*], Sushil Bhargav[2]

[1]Department of Pharmaceutical Chemistry, Apollo College of Pharmacy, Anjora Durg, Chhattisgarh, INDIA.
[2]Department of Pharmacy, Faculty of Pharmaceutical Sciences, Madhav University, Abu Road Pindwara, Rajasthan, INDIA.

ABSTRACT

Background: *O. carniculata* contains bioactive substances called C-glycosyl-flavones that have antioxidant and anti-inflammatory properties. The inhibitory effect of C-glycosyl-flavones of *O. carniculata* on MMPs was established by *in silico* molecular modeling approach, that are linked to the collagen degradation pathway. **Materials and Methods:** Structural flexibility, binding-conformation, binding-free energy, and protein-ligand-interaction profile of Matrix Metalloproteinases (MMPs): MMP1 (966C), MMP3 (1G4K), and MMP9 (1GKC) were established using molecular docking, induced fit docking and pharmacophore mapping to understand the structural basis of three C-glycosyl-flavones, viz Isoorientin (6-C-glucosyl-lutein), Isovitexin (6-C-glucosyl-apigenin) and Swertisin (7-methylether-isovitexin), for their potential as MMP inhibitor. Additionally, the e-pharmacophore model for MMP inhibitors has been developed in a way that efficiently mapped all of the crucial pharmacophoric attributes associated with the MMP inhibitory activity. **Results and Discussion:** Isoorientin and Isovitexin showed the greatest binding affinity to the MMPs among the three C-glycosyl-flavones. The e-pharmacophores had three (for 966C) and, six (for 1G4K and 1GKC) featured models and all showed good fitness score (ranging from 1.42 to 1.49) These results demonstrate that the Isoorientin has the greatest potential for use as an anti-skin-aging agent with the MMP inhibitory activity.

Keywords: MMP, Molecular docking, Phytochemicals, Induced fit docking, Pharmacophore.

Correspondence:
Dr. Madhuri Baghel
Professor and Principal, Department of Pharmaceutical Chemistry, Apollo College of Pharmacy, Anjora Durg-491001, Chhattisgarh, INDIA.
Email: banchhormadhuri@gmail.com

Received: 12-01-2026;
Revised: 25-02-2026;
Accepted: 07-04-2026.

INTRODUCTION

MMPs (Matrix Metalloproteinases) have emerged as an important drug targets for the discovery of potent inhibitors.[1] MMPs belong to a family of $Zn^{2+}$and Ca^{2+}containing proteins.[2,3] Molecule that efficiently inhibit the polypeptide from binding to MMPs, have high affinity for Zn^{2+} and are regarded as MMP inhibitors.[4] MMPs are essential for remodeling ECM (extracellular matrix) structures in a number of pathological conditions, including inflammation, carcinogenesis, wound healing, and dermal photoaging.[5,6] In terms of the photoaging, ROS (reactive oxygen species) are formed when UVB rays penetrate the epidermis,[7] which triggers cell surface receptors, stimulates MAPK (mitogen-activated-protein-kinase) cascades, and promotes the expression of pro-inflammatory cytokines like TNFα, IL1, IL6, and IL-8. These cytokines in turn provoke the expression of c-Fos and c-Jun that forms a nuclear-transcription-factor-complex, and AP1 (activator protein1) and NFκB (nuclear factor kappa B). In human skin keratinocytes and fibroblasts, increases the production and release of matrix degrading enzymes MMPs, such as Collagenase (MMP1), stromelysin-1 (MMP3), and gelatinase (MMP9), and they inhibit type I procollagen.[8,9] MMP1 initiates fibrillar collagen cleavage inside the central triple helix (collagen I and III) in the skin. Collagen is now degraded by the increased levels of MMP3 and MMP9 after being cleaved by this enzyme.[10] Inhibiting MMP and AP1 activity directly and competitively might be a sensible therapeutic strategy, especially for preventing and managing UV induced photoaging.

In recent years, plant bioactives have drawn a lot of attention for hindering skin photodamage brought on by UV radiation.[3] *O. carniculata*, also known as creeping wood sorrel, is a member of the Oxalidaceae family.[11,12] Along with flavonoids, the major bioactive compounds of *O. carniculata* consist of terpenoids, alkaloids, steroids, phlobatannins, saponins, and cardiac glycosides. It has been demonstrated to possess a variety of biological activities, including antibacterial, anti-fungal, anti-cancer, anti-diabetic, cardioprotective, wound healing and anti-oxidant, due to its flavonoid, polyphenolic, and

DOI: 10.5530/ijper.20266452

glycosides profile.[13-15] Leaves consists of citric acids, tartaric acid, calcium oxalate, glycoflavones (4'-O-methyl-vitexin, 4'-O-methyl-isovitexin and 3',4'-di-O-methyl- orientin), flavones (acacetin and 7,4'-di-O-methyl-apigenin), flavonols (3',4'-di-O-methyl-quercetin) and phenolic acids viz syringic, p-hydroxybenzoic, and vanillic acid. Further studies revealed the presence of three important C-glycosylflavones in *Oxalis* leaves, these are isovitexin (6-C-glucosyl-apigenin), isoorientin (6-C-glucosyl-lutein), and swertisin (7-methylether-isovitexin) (Figure 1).[16,17] Recent studies by Sachin Gudasi *et al* on the cytotoxic and antioxidant potential of *Oxalis Corniculata* on the Hep-G2 (human hepatocarcinoma) cell line and molecular docking studies of some phytocompounds have been reported.[17]

In the present investigation, an *in silico* approach was employed to examine the potential inhibitory properties of Isoorientin, Isovitexin, and Swertisin on the MMP activity. The binding mechanism of phytochemicals from *O. carniculata* in the binding region of MMPs was thus revealed by experiments using molecular docking, induced fit docking and Pharmacophore mapping which resulted in a diminution of UV-induced skin ageing. Additionally, a known and broad spectrum MMP inhibitor, Batimastat.[12] was docked against MMP receptors for comparison that have IC_{50} values of 10nM, 20nM, and 1nM against MMP1, MMP3, and MMP9, respectively.

MATERIALS AND METHODS

Protein Preparation

The 3D structures of photoaging-related MMPs were retrieved from RCSB with PDB ids 966C (MMP-1,1.9 Å resolution),[18] 1G4K at (MMP-3,2.0 Å resolution)[19] and 1GKC (MMP9,2.3 Å resolution).[20] From the protein preparation wizard, 3D crystal structures of downloaded proteins were prepared. Bond orders were allocated, hydrogens were added, zero bonds to disulfide and metal bonds were chosen and het states were set at pH 7.0±2.0.[21] The crystallographic water outside 3.0 A^0 from het, was deleted from the protein before performing the docking studies. H-bond networks were optimised using PROPKA in the refine tab.[22] In order to eliminate any potential stearic clashes in the structure, the retrained minimization was performed using the OPLS5 force field.

Ligands selection and preparation of MMP inhibitors

Three C-glycosylflavones of *O. carniculata* reported in literature were retrieved from PubChem (Figure 1), these are Isoorientin (CID-114776), Isovitexin (CID-162350), Swertisin (CID-124034). Schrodinger Maestro suite's LigPrep module was utilized to all ligands in their 3D structure format. Stereo-chemistries, desalting, and tautomer generation were chosen to obtain at least 32 conformations for each ligand as they were optimized using Epik in pH between 7±2.

Receptor grid generation and molecular docking (Rigid and Flexible)

With the help of the Schrödinger suite's glide Grid-based ligand docking programme, the grid was created around the co-crystallized structure. In this study, rigid and flexible docking was carried out using the Maestro12.8 version tool to estimate the binding affinities, ligand efficacy, and inhibitory constant to the targets. Glide XP (Extra precision) mode, was used to dock the ligands to the active binding site of MMPs.[23] Induced Fit Docking (IFD) protocol was used to precisely predict the affinity of MMP inhibitors for binding to protein crystals using Glide and the Refinement module in Prime.[24]

Pose Validation

By redocking the co-crystallized ligand into the proteins' active sites, the reproducibility of this computational technique was assessed and confirmed. The RMSD (root mean square deviation) of the bound ligands were found to be 1.473Å, 1.324Å and 0.932 for MMP1, 3 and 9, respectively. This confirms that the docking protocol is reproducible.

Prime MM-GBSA (molecular-mechanics -generalized-born surface area) calculations

Using the MM-GBSA module in the Schrodinger Suite 2021, the ligand binding energy for all of the three phytochemicals and the standard suggested for inhibiting MMP was calculated.[25] This post-docking tool is essential since it reveals the right ranking of ligands binding and help to predict the relative free binding energy with an acceptable level of accuracy. Here, the free binding energies of the complexes docked using the XP docking methods were determined using the PRIME module incorporated into Maestro.

e-Pharmacophore (energy-optimized-pharmacophore) Generation

The e-pharmacophore feature uses the Glide XP scoring function for mapping the energetic terms retrieved from docking calculations to the atom centres. The co-crystallized ligand in the MMP inhibitor complex determined by the Glide XP docking calculations was used to construct pharmacophore sites utilising a default set of six chemical features: R (aromatic ring); H (hydrophobic site); D (hydrogen-bond donor); A (hydrogen-bond acceptor), N(negative-ionizable group) and P(positive-ionizable group). These sites were created through the Phase module.[26]

RESULTS

The XP and IFD scores (Table 1) of investigated phytochemicals with MMPs revealed that for protein target 966C; Swertisin generated highest binding affinity with glide XP docking score of -8.572kcalmol^{-1} which is significantly higher than the reference compound Batimastat (-6.437kcalmol^{-1}). With regard

to the IFD results, Isoorientin had the best score (-6193.36 kcalmol^{-1}), followed by Isovitexin (-6177.33 kcalmol^{-1}) and Swertisin (-6172.17 kcalmol^{-1}). The IFD scores for all three phytochemicals were considerably higher than Batimastat (-6115.46 kcalmol^{-1}). Similarly, the MM-GBSA binding score was highest for Isoorientin (-44.75kcalmol^{-1}), then for Isovitexin (-43.83kcalmol^{-1}) and Swertisin (-41.51kcalmol^{-1}). In comparison to Batimastat (-7.65 kcalmol^{-1}) MM-GBSA binding score, all phytochemicals displayed much higher scores.

Similarly, Isovitexin showed the highest binding affinity for the target protein 1GKC (-6.142 kcalmol^{-1}), which is higher than the reference value of -5.134 kcalmol-1. Swertisin and Isoorientin came in second and third, respectively, with glide XP docking scores of -5.187 kcalmol^{-1} and -5.068 kcalmol^{-1}. The results of induced fit docking, however, indicated that Isoorientin, Isovitexin and Swertisin showed the most favorable scores of -5508.21kcalmol^{-1}, 5474.92 kcalmol^{-1} and 5464.17 kcalmol^{-1} respectively for Isoorientin, Isovitexin and Swertisin respectively, which was higher than the IFD score generated for Batimastat (-5012.80kcalmol^{-1}). It's interesting to note that all phytochemicals outperformed the reference (48.31kcalmol^{-1}) in terms of MM-GBSA binding score.

Batimastat (-6.775kcalmol^{-1}) recoded significantly higher XP binding score as compared to all three phytochemicals for the protein target 1G4K. The highest rating among these phytochemicals have been assigned to isoorientin (-4.930 kcalmol^{-1}), followed by isovitexin (-4.628 kcalmol^{-1}) and swertisin (-4.473 kcalmol^{-1}). Intriguingly, compared to the reference (-4551.55 kcalmol^{-1}), all three phytochemicals had higher binding affinity, with IFD scores of -5185.29 kcalmol^{-1}, -5168.57 kcalmol^{-1}, and -5166.63 kcalmol^{-1}, respectively. All three phytochemicals (-66.09 kcalmol^{-1} for Isoorientin, -56.02 kcalmol^{-1} for Isovitexin, and -53.64 kcalmol^{-1} for Swertisin) were found to have higher MM-GBSA binding affinities than the reference (-35.99 kcalmol^{-1}). 2D interactions, IFD poses (top ten) and fingerprint analysis of phytochemicals with protein 966C, 1GKC and 1G4K is illustrated in Figure 2a and b.

e-Pharmacophore

By using Glide XP docking, the e-pharmacophores has been generated in this study using high resolution crystal structures of 966C, 1G4K, and 1GKC in complex with N-Hydroxy-2[4(4-phenoxy-benzenesulfonyl)-tetrahydro-pyran-4-yl]acetamide, Stromelysin-1, and N~2~-[(2R)-2-{[formyl(hydroxy)amino]methyl}-4-methylpentanoyl]-N,3-dimethyl-L-valinamide respectively by considering the structural and interactional energy information between the MMP and the co-crystal ligands, so that all of the Glide XP energetic terms were assigned on to the atoms. The created e-pharmacophores were used to screen the phytochemical after being validated through enrichment studies.

DISCUSSION

The development and fabrication of novel therapeutics heavily relies on molecular docking approaches. They attempt to accurately predict a native molecule's experimental binding mode and affinity within the drug target's binding site. MMP is a crucial enzyme that contributes significantly to skin ageing. They act as a mediator in the degeneration of the various ECM components as well. MMPs (MMP1, 3, and 9) and the functions of their natural inhibitors, Tissue Inhibitor of Metalloproteinases (TIMPs), normally control the degradation of collagen.

All phytochemicals interacted with Zn 265; Isoorientin formed similar metal co-ordination bond as with the reference compound Batimastat, while Isovitexin and Swertisin interacted via Pi-Pi cataion with Zn 265 residue. Both Batimastat and

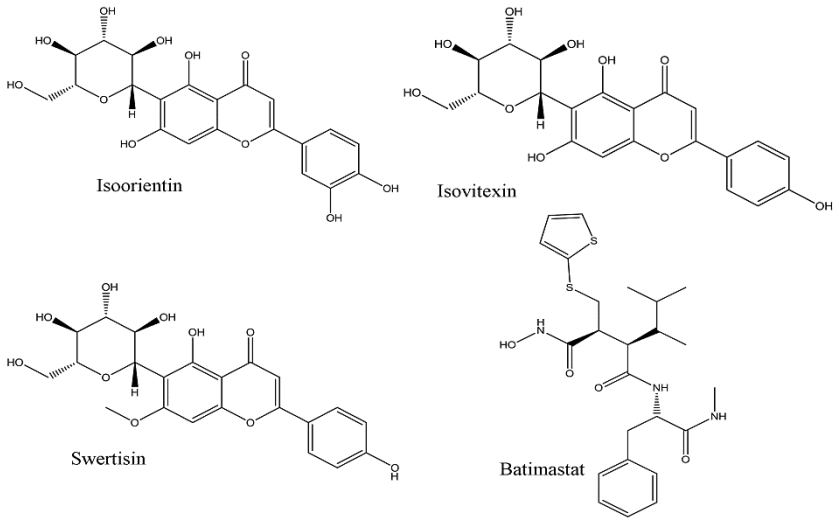

Figure 1: Chemical structure of phytochemicals and standard.

Isoorientin forms H-bond with the amide nitrogen and ALA 182 residue. Isoorientin formed five additional H-bonds with Zn 265, HIS 218, ASN 180, THR 241 and THR 237 residue, while Batimastat formed two additional H-bonds with LEU 181 and GLY 179 residue. Isovitexin formed bridged H-bond with ALA 182 involving carbonyl oxygen and hydroxyl group. Additionally, it formed Pi-Pi stacking with HIS 218 involving Phenyl ring of phytochemical. It also formed H-bond with oxane ring and ASN 180 residue. Swetisin formed H-bond with THR 241 and ASN 180.

Table 1: Docking score, induced fit docking, MMGBSA score, interacting residue and type of interaction of phytochemicals and reference with MMPs (966C, 1G4K, 1GKC).

Protein with pdb code	CID and compound name	XP Docking score	IFD score	MMGBSA d G bin d (kcalmol^{-1})	Residues interactions	Types of bond formation
MMP1 (966C)	114776 (Isoorientin)	-6.451	-6193.36	-44.75	Zn 265 Zn 265 ALA 182 HIS 218 ASN 180 THR 241 THR 237	Metal coordination bond with hydroxyl Salt bridge with carboxlate ion H-Bond with amide nitrogen H-Bond with amide oxygenH-Bond with amide nitrogen H-Bond bond with hydroxyl H-Bond bond with hydroxyl H-Bond bond with hydroxyl
	162350 (Isovitexin)	-6.412	-6177.33	-43.83	Zn 265 ALA 182 HIS 218 ASN 180	Pi cataion with Phenyl ring H-Bond with amide nitrogen H-Bond with carbonyl oxygen and hydroxy Pi-Pi stacking with Phenyl ring H-Bond with Oxane ring and hydroxy
	124034 (Swertisin)	-8.572	-6172.17	-41.51	Zn 265 THR 241 ASN 180	Pi cataion with Phenyl ring H-Bond with hydroxy H-Bond with withhydroxy
	5362422 (Reference-Batimastat)	-6.437	-6115.46	-7.65	Zn 265 ALA 182 LEU 181 GLY 179	Metal coordination bond with hydroxyl and carbonyl group H-Bond with amide nitrogen H-Bond with amide oxygen H-Bond with amide nitrogen
MMP3 (1G4K)	114776 (Isoorientin)	-4.930	-5185.29	-66.09	Zn 301 HIS 201 HIS 201 TYR 223 ASN 162 TYR 220	Metal coordination bond carbonyl oxygen Pi-Pi stacking with Phenyl ring Pi-Pi stacking with Oxane ring Pi-Pi stacking with Phenyl ring H-Bond with hydroxyl H-Bond with carbonyl oxygen
	162350 (Isovitexin)	-4.628	-5168.57	-56.02	Zn 301 HIS 201 HIS 201 TYR 223 ASN 162	Metal coordination bond carbonyl oxygen Pi-Pi stacking with Phenyl ring Pi-Pi stacking with Oxane ring Pi-Pi stacking with Phenyl ring H-Bond with hydroxyl
	124034 (Swertisin)	-4.473	-5166.63	-53.64	--	--
	5362422 (Reference-Batimastat)	-6.775	-4551.55	-35.99	Zn 301 GLH 202 ALA 165 HIS 201 TYR 223	Metal coordination bond carbonyl oxygen H-Bond with hydroxyl H-Bond with hydroxyl Pi-Pi stacking with thiophene H-Bond with carbonyl oxygen

MMP9 (1GKC)	114776 (Isoorientin)	-5.068	-5508.21	-51.43	Zn 1450	Metal coordination bond
					ASP 182	H-Bond with hydroxyl
					HIS 401	Pi-Pi stacking with Phenyl ring
					HIS 401	Pi-Pi stacking with Oxane ring
					HIS 186	H-Bond with hydroxyl
					TYR 420	H-Bond with hydroxyl
					TYR 423	Pi-Pi stacking with Phenyl ring
	162350 (Isovitexin)	-6.142	-5474.92	-54.74	ALA 189	H-Bond with hydroxyl
					LEU 188	H-Bond with hydroxyl
					GLH 402	H-Bond with hydroxyl
					TYR 423	H-Bond with hydroxyl
	124034 (Swertisin)	-5.187	-5464.17	-48.58	TYR 423	Pi-Pi stacking with Phenyl ring
					HIS 401	Pi-Pi stacking with Oxane ring
					HIS 401	Pi-Pi stacking with Phenyl ring
					PRO 421	H-Bond with water molecule
	5362422 (Reference-Batimastat)	-5.134	-5012.80	-48.31	Zn 1450	Metal coordination bond
					PRO 421	H-Bond with amide nitrogen
					TYR 423	Pi-Pi stacking with thiophene
					TYR 423	H-Bond with carbonyl oxygen
					TYR 393	H-Bond with amide nitrogen
					GLY 186	H-Bond with amide nitrogen

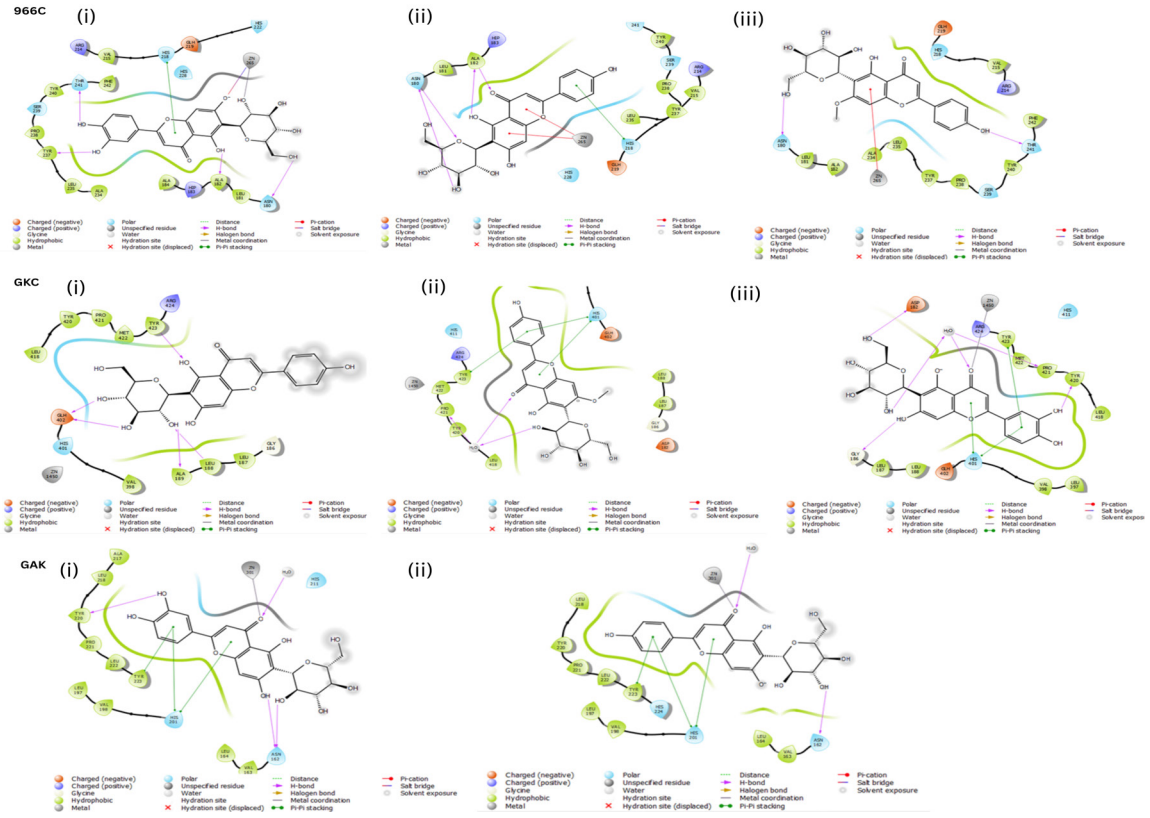

Figure 2a: 2 D interaction of Phytochemicals with the protein 966C, 1GKC and 1G4K i) Isoorientin ii) Isovitexin iii) Swertisin.

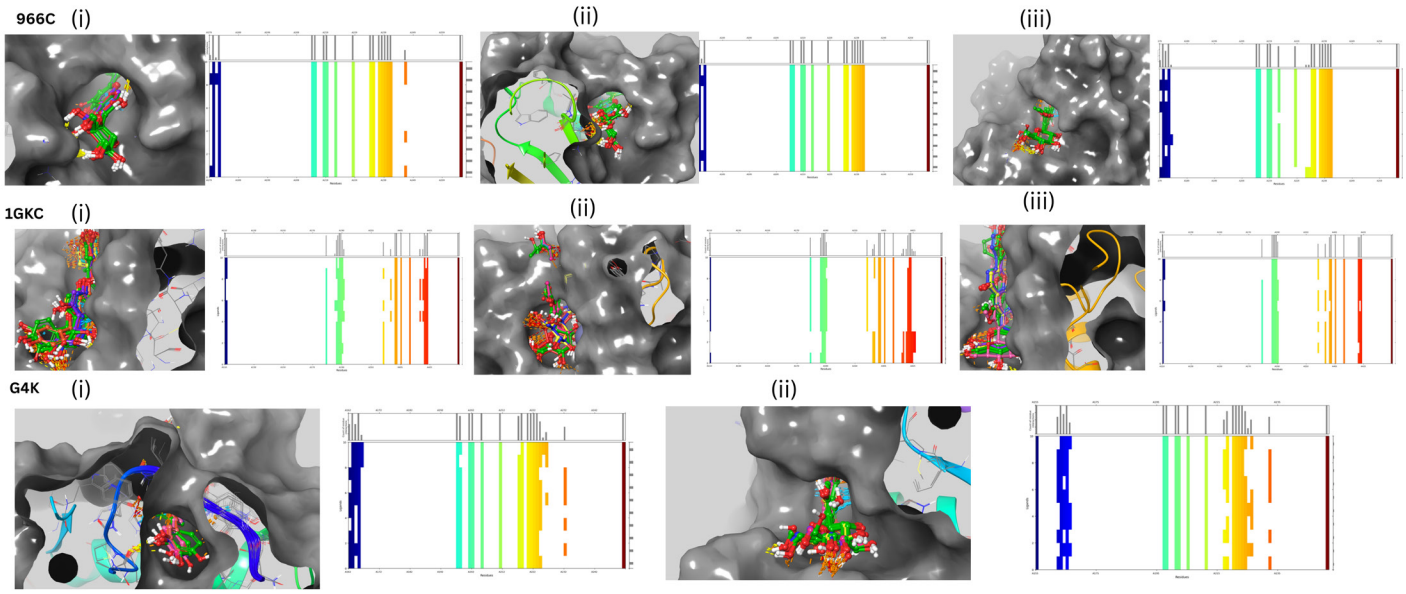

Figure 2b: overlay and fingerprint analysis (Showing consistent interactions) of top 10 poses of IFD for protein 966C, 1GKC and 1G4K i) Isoorientin ii) Isovitexin iii) Swertisin.

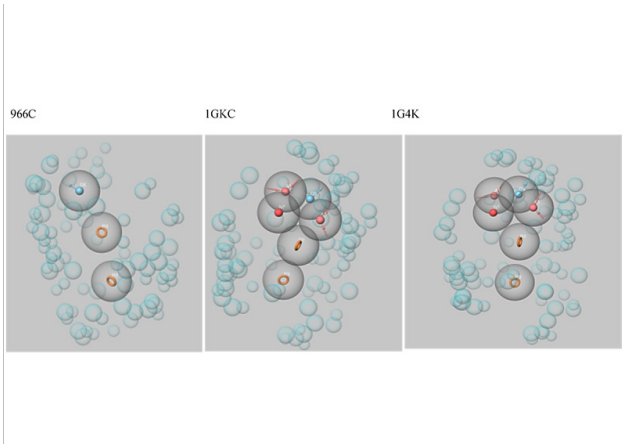

Figure 3: Pharmacophoric features for 966C, 1GKC and 1G4K.

With respect to protein 1GKC, the reference compounds and Isoorientin formed metal co-ordination bond with Zn 1450 residue. Both also showed pi-pi stacking with the TYR 423 residue. Additionally, Isoorientin formed three H-bonds with ASP 182, HIS 186 and TYR 420 residue, while Batimastat formed H-bonds with PRO 421, GLY 186, TYR 393 and TYR 423 residue. Isovitexin and Swertisin did not interacted with Zn residue but Isovitexin formed four H-bonds (with ALA 189, LEU 188, GLH 402, TYR 423) and swertisin formed three pi-pi stacking interactions (TYR 423, HIS 401 with both oxane and phenyl ring) respectively.

For protein 1G4K, Isoorientin, Isovitexin and Batimastat showed similar interaction with Zn 301 and TYR 223 residue. Additionally, reference formed H-bonds (with GLH202, ALA165) and showed pi-pi stacking interaction (HIS 201), while Isoorientin formed H-bonds with ASN 162, TYR 220 residue and pi-pi stacking interaction with HIS 201. Isovitexin also formed H-bonds with ASN 162 residue and pi-pi stacking interaction with HIS 201. Interestingly no interactions were observed with Swertisin.

Based on the pharmacophoric features (Figure 3), each e-pharmacophore has a different screening efficiency. The resulting e-pharmacophores had three and, six featured models with pharmacophoric sites, AAD for 966C, AAAAND for both 1G4K and 1GKC. Good fitness were recorded for 966c, for all the three phytochemicals ranging from 1.89 to 1.99 with 100% pharmacophoric feature match, while the fitness score for reference was quite low (0.419) with 66% match. For 1G4K all the compounds including reference showed good fitness score ranging from 1.42 to 1.49. Isoorientin and Isovitexinn showed 100% match while swetisin and reference showed 83% and 66% match. For 1GKC the fitness score ranges from 0.93 to 1.22 with 100% match, for phytochemicals while the reference

recorded higher fitness score (1.672, with 83% match) than the phytochemicals.

CONCLUSION

Increased MMP levels trigger photo-degeneration and skin ageing. *In silico* analyses of phytochemicals from *O. carniculata* have been utilised in developing MMP inhibitors with effective protecting ability against the photo-induced skin ageing due to the accessible and well resolved crystallographic structures of MMPs. The currently implemented molecular docking, induced fit docking, and pharmacophore modelling study offers important insights into the inhibition of activity of the photoaging-related proteins MMP1, MMP3, and MMP9, which may provide skin protection against UV-induced skin ageing process. All the three phytochemicals were predicted to be more potent than the standard MMP inhibitor Batimastat. Among the three C-glycosyl-flavones studied Isoorientin was found to be best in terms of Glide docking score, IFD score and MMGBSA binding score for all the three proteins (966C, 1G4K and 1GKC). Although swertsin showed better docking score for 966C and Isovitexin showed better docking score for 1GKC. Similarly, the results of pharmacophore mapping recorded best match and fitness score for Isoorientin for 966C and 1GKC, while swertisin was best for 1G4K. The results of these studies provide new perspective with regard to investigation of interaction of phytochemicals with specific proteins and they enable us to identify one or most promising bioactive compounds to be isolated for *in vitro* and *in vivo* tests in a subsequent study.

ACKNOWLEDGEMENT

The authors wish to thank Chhattisgarh Swami Vivekanand Technical University, Bhilai, CG for providing software facility.

CONFLICT OF INTEREST

The authors declare that there is no conflict of interest.

ABBREVIATIONS

MMPs: Matrix metalloproteinases; **ECM:** Extracellular matrix; **ROS:** Reactive Oxygen Species; **MAPK:** Mitogen-activated-protein-kinase; **AP1:** Activator protein1; **NFκB:** nuclear factor kappa B; **Hep-G2:** Human hepatocarcinoma; **MM-GBSA:** Molecular-mechanics-generalized-born surface area; **e-Pharmacophore:** Energy-optimized-pharmacophore.

REFERENCES

1. Saur IML, Panstruga R, Schulze-Lefert P. NOD-like receptor-mediated plant immunity: from structure to cell death. Nat. Rev. Immunol. 2021;21(5):305-18.
2. Skiles JW, Gonnella NC, Jeng AY. The Design, Structure, and Clinical Update of Small Molecular Weight Matrix Metalloproteinase Inhibitors. Curr. Med. Chem. 2012; 11(22):2911-77.
3. Baghel M, Badwaik H, Patil S, Azajuddin A. Plant Bioactives as Inhibitors of Matrix Metalloproteases and their Anti-skin Photoaging Potential. Pharmacogn. Rev. 2022;16(32):126-38.
4. Tu GG,Xu WF,Huang HM,Li SH. Progress in Development of Matrix Metalloproteinase Inhibitors. Curr. Med. Chem., 2001;15(14):1388-95.
5. Hu J, Van den Steen PE, Sang QXA, Opdenakker G. Matrix metalloproteinase inhibitors as therapy for inflammatory and vascular diseases. Nat. Rev. Drug Discov. 2007: 6(6): 480-98.
6. Kim J, Lee CW, Kim EK, Lee SJ, Park NH, Kim HS, Kim HK, Char K, Jang YP, Kim JW, Inhibition effect of *Gynura procumbens* extract on UV-B-induced matrix-metalloproteinase expression in human dermal fibroblasts. J. Ethnopharmacol. 2011; 137: 427-33.
7. Philips N, Auler S, Hugo R, Gonzalez S. Beneficial regulation of matrixmetalloproteinases for skin health. Enzyme Res. 2011: 11: 4272-85.
8. Jung HY, Shin JC, Park SM, Kim NR, Kwak W, Choi BH. Pinus densiflora extract protects human skin fibroblasts against UVB-induced photoaging by inhibiting the expression of MMPs and increasing type I procollagen expression. Toxicol. Reports. 2014: 11: 658-66.
9. Park M, Han J, Lee CS, Heung Soo B, Lim KM, Ha H. Carnosic acid, a phenolic diterpene from rosemary, prevents UV-induced expression of matrix metalloproteinases in human skin fibroblasts and keratinocytes. Exp. Dermatol. 2013: 22(5): 336-41.
10. Kim EM, Hwang O. Biochemical characteristics of MMP-3 Regulation of MMP-3 transcription. J. Neurochemistry. 2011: 116:22-32.
11. Sarkar T, Ghosh P, Poddar S, Sarkar A, Chatterjee S. *Oxalis corniculata* Linn. (Oxalidaceae): A brief review. J. Pharmacogn. Phytochem. 2020; 9(4): 651-55.
12. Singh T, Adekoya OA, Jayaram B. Understanding the binding of inhibitors of matrix metalloproteinases by molecular docking, quantum mechanical calculations, molecular dynamics simulations, and a MMGBSA/MMBappl study. Mol. Biosyst. 2015: 11(4): 1041-51,.
13. Sarfraz I, Rasul A, Hussain G, Shah MA, Nageen B, Jabeen F, Selamoğlu Z, Ucak I, Asrar M, Adem S. A Review on Phyto-pharmacology of *Oxalis corniculata*. Comb. Chem. High Throughput Screen. 2021; 25(7): 1181-86.
14. Karunanithi S, Rajkishore VB, Pol VG, Abirami SMMD, Jayshree D. Pharmacognostical and phytochemical studies on leaves of *Oxalis corniculata* Linn. J. Phytopharm. 2016; 5(6): 225-29.
15. Kaur S, Kaur G, Singh J. Phytochemical screening and biological potential of methanolic extract of *Oxalis corniculata* using different parts of plant. Res. J. Chem. Sci. 2017;7(7): 26-32.
16. Srikanth M, Swetha T, Veeresh B. Phytochemistry and Pharmacology of *Oxalis Corniculata* Linn: A Review. International Journal of Pharmaceutical Sciences and Research. 2012; 11: 4077-85.
17. Gudasi S, Gharge S, Koli R, Patil K. Antioxidant properties and cytotoxic effects of *Oxalis corniculata* on human Hepatocarcinoma (Hep - G2) cell line : an *in vitro* and *in silico* evaluation. Futur. J. Pharm. Sci. 2023; 9: 25-29.
18. Lovejoy B, Welch AR, Carr S, Luong C, Broka C, Hendricks T, Campbell JA, Walker KAM, Martin R, Wart HV, Browner MF. Crystal structures of MMP-1 and -13 reveal the structural basis for selectivity of collagenase inhibitors. Nat. Struct. Biol. 1999; 6(3): 23-31.
19. Dunten P, Kammlott U, Crowther R, Levin W, Foley LH, Wang P, Palermo R. X-ray structure of a novel matrix metalloproteinase inhibitor complexed to stromelysin. Protein Sci. 2001; 10(5): 92326.
20. Rowsell S, Hawtin P, Minshull CA, Sarah HJ, Barratt, MV, Slater AM, McPheat WL, Waterson D, Henney AM, Pauptit RA. Crystal structure of human MMP9 in complex with a reverse hydroxamate inhibitor. J. Mol. Biol. 2002; 319(1):173-81.
21. Schrödinger Release 2021-2: LigPrep, Schrödinger, LLC, New York, NY, 2021.
22. Olsson MHM, Sondergaard CR, Rostkowski M, Jensen JH. PROPKA3: Consistent treatment of internal and surface residues in empirical pKa predictions. J. Chem. Theory Comput. 2011: 7(2): 525-37.
23. Schrödinger Release 2021-2: Desmond, Schrödinger, LLC, New York, NY, 2021.
24. Sherman W, Day T, Jacobson MP, Friesner RA, Farid R. Novel procedure for modeling ligand/receptor induced fit effects. J. Med. Chem. 2006; 49(2): 534-53.
25. Schrödinger Release 2021-2: Prime, Schrödinger, LLC, New York, NY, 2021.
26. Schrödinger Release 2021-2: Phase, Schrödinger, LLC, New York, NY, 2021.

Cite this article: Baghel M, Bhargav S. Investigation of Potential of *Oxalis corniculata* through Inhibition of Matrix Metalloproteinases for the Treatment of Skin Photoageing: An *in silico* Approach. Indian J of Pharmaceutical Education and Research. 2026;60(3):1199-205.